REPORT 933

PERFORMANCE OF CONICAL JET NOZZLES IN TERMS OF FLOW AND VELOCITY COEFFICIENTS

By Ralph E. Grey, Jr. and H. Dean Wilsted

SUMMARY

Performance characteristics of conical jet nozzles were determined in an investigation covering a range of pressure ratios from 1.0 to 2.8, cone half-angles from 5° to 90°, and outlet-inlet diameter ratios from 0.50 to 0.91. All nozzles investigated had an inlet diameter of 5 inches.

The flow coefficients of the conical nozzles investigated were dependent on the cone half-angle, outlet-inlet diameter ratio, and pressure ratio. The velocity coefficients were essentially constant at pressure ratios below the critical. For increasing pressures above critical pressure ratio, there was a small decrease in velocity coefficient that was dependent on pressure ratio and independent of cone half-angle and outlet-inlet diameter ratio. Therefore the variation in performance (air flow and thrust) of several nozzles, selected for the same performance at a particular design condition, was proportional to the ratio of their flow coefficients.

INTRODUCTION

A correctly designed jet nozzle as a device for converting pressure energy to kinetic energy is an essential part of an efficient jet-propulsion power plant. Current jet power plants utilize, with but few exceptions, the conical subsonic jet nozzle because it is simple, inexpensive to fabricate, and the configuration is inherently strong and rigid.

In the design of jet nozzles, it has been necessary in the past to use approximate velocity and discharge coefficients. This necessity, coupled with the effects of other engine-design uncertainties, often requires changes in the design of the jet nozzle during prototype-power-plant tests. Exact nozzle-performance data would enable a more rational process of selecting a nozzle to perform a specific task and would also enable the designer to predict more accurately power-plant performance over the complete operating range.

Performance characteristics of 15 conical nozzles were experimentally determined at the NACA Lewis laboratory in the early part of 1947 and are presented herein. The nozzle configurations investigated have outlet-inlet diameter ratios ranging from 0.50 to 0.91 and cone half-angles ranging from 5° to 90°. All the nozzles have inlet diameters of 5 inches. For each configuration, the pressure ratio was varied between 1.0 and 2.8. For convenience, outlet-inlet diameter ratio and cone half-angle are hereinafter referred to as "diameter ratio" and "cone angle," respectively.

The results of this investigation should be useful for the design of or for the determination of the performance of conical jet-propulsion nozzles. Factors relating to flow similarity are considered to aid in determining the validity of applying these results to other conical-nozzle uses.

SYMBOLS

The following symbols are used in this report:

A	cross-sectional area, (sq ft)
C_d	flow (discharge) coefficient, W_m/W_t
$C_{v,e}$	effective velocity coefficient, V_e/V_t
C_v	velocity coefficient, V_m/V_t
c_p	specific heat at constant pressure, (Btu/(lb)(° F))
D	diameter, (ft)
F_j	jet thrust, (lb)
g	acceleration due to gravity, 32.17 (ft/sec^2)
J	mechanical equivalent of heat, 778 (ft-lb/Btu)
M	Mach number
m	mass, (slugs)
P	total pressure, (lb/sq ft)
p	static pressure, (lb/sq ft)
R	gas constant, 53.3 (ft-lb/(lb)(° F))
Re	Reynolds number
T	total temperature, (° R)
T_i	indicated temperature, (° R)
t	static temperature, (° R)
V	jet velocity, (ft/sec)
V_e	effective jet velocity, (ft/sec)
W	fluid flow, (lb/sec)
α	jet-nozzle cone half-angle, (deg)
β	thermocouple impact-recovery factor
γ	ratio of specific heat at constant pressure to specific heat at constant volume
μ	viscosity, (lb/(sec)(ft))
ρ	fluid density, (lb/cu ft)
τ	time, (sec)

Subscripts:

m	measured value
t	theoretical value
x	example nozzle 1
y	example nozzle 2
0	ambient
1	jet-nozzle inlet
2	jet-nozzle outlet

A prime indicates conditions of critical (sonic) flow in the nozzle outlet (throat).

ANALYSIS

In order to design a nozzle for a specific application, two performance characteristics are generally required: the flow capacity, and the effectiveness of converting pressure energy to kinetic energy or velocity. Flow capacity and effectiveness of energy conversion are evaluated in terms of flow coefficient C_d and velocity coefficient C_v, respectively, which are defined as

$$C_d=\frac{W_m}{W_i} \tag{1}$$

and

$$C_v=\frac{V_m}{V_i} \tag{2}$$

The evaluation of these coefficients is based on the temperatures and the pressures at stations 1 and 0 in the following sketch:

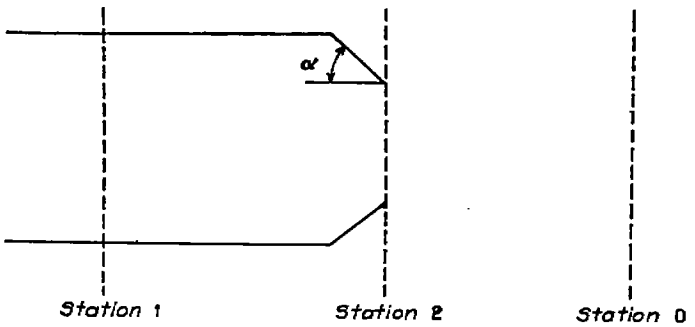

These quantities are usually available for jet-propulsion or ejector nozzles. The evaluation is based on one-dimensional compressible-flow equations, so that the coefficients obtained may be easily applied. Inasmuch as the pressure distribution in the plane of the jet-nozzle outlet (station 2) is generally unknown, the discharge pressure is assumed to be atmospheric for subcritical pressure ratios. For supercritical pressure ratios the fluid is assumed to expand only to the critical pressure, which is the discharge pressure that will just produce sonic velocity in the nozzle throat. The critical pressure can be determined by differentiating the equation for mass flow through a nozzle with respect to the downstream static pressure p_2 and setting the result equal to zero. This operation gives

$$\frac{p_2}{P_1}=\left(\frac{2}{\gamma+1}\right)^{\frac{\gamma}{\gamma-1}} \tag{3}$$

The actual jet velocity $V_{m,2}$ was obtained from the jet thrust in the following manner: The equation for jet thrust for subcritical pressure ratios can be written from Newton's second law of motion as

$$F_j=m\frac{dV_m}{d\tau} \tag{4}$$

which states that the force is equal to the rate of change of momentum. Then, if the fluid is assumed to start from rest (stagnation conditions at station 1), this equation may be rewritten as

$$F_j=\frac{W_m}{g}V_{m,2}=\frac{C_dW_i}{g}C_vV_{i,s} \tag{5}$$

The theoretical jet velocity may be derived from the conservation-of-energy equation

$$\frac{(V_{i,1})^2}{2gJc_p}+t_1=\frac{(V_{i,2})^2}{2gJc_p}+t_2=T_1 \tag{6}$$

If the change in c_p is assumed to be negligible between T_1 and t_2,

$$V_{i,2}=\sqrt{2gJc_p(T_1-t_2)} \tag{7}$$

The temperature at the nozzle outlet can be determined from the isentropic-expansion expression

$$t_2=T_1\left(\frac{p_2}{P_1}\right)^{\frac{\gamma-1}{\gamma}} \tag{8}$$

Then equation (7) becomes

$$V_{i,2}=\sqrt{2gJc_pT_1\left[1-\left(\frac{p_2}{P_1}\right)^{\frac{\gamma-1}{\gamma}}\right]} \tag{9}$$

The weight flow at any section may be expressed by the continuity-of-flow equation and at station 2 may be written as

$$W_i=\rho_{i,2}A_2V_{i,2} \tag{10}$$

From the gas law and the isentropic relation, and for subsonic flow with $p_2=p_0$ assumed,

$$\rho_{i,2}=\frac{p_2}{Rt_2}=\frac{p_0}{RT_1}\left(\frac{P_1}{p_0}\right)^{\frac{\gamma-1}{\gamma}} \tag{11}$$

Substituting this value of $\rho_{i,2}$ in equation (10) gives

$$W_i=A_2\frac{p_0}{RT_1}\left(\frac{P_1}{p_0}\right)^{\frac{\gamma-1}{\gamma}}V_{i,2} \tag{12}$$

in which $V_{i,2}$ may be evaluated by equation (9).

For supercritical pressure ratios, there is an excess of pressure (p_2-p_0) beyond that converted to velocity. The pressure at the nozzle outlet p_2 may be computed from equation (3). For supercritical pressure ratios, equation (5) then becomes

$$\begin{aligned}F_j&=\frac{W_m}{g}V_2+A_2(p_2-p_0)\\&=C_d\frac{W_i'}{g}C_vV_{i,2}'+A_2(p_2-p_0)\end{aligned} \tag{13}$$

Critical or supercritical pressure ratios across the nozzle establish sonic velocity and the maximum flow obtainable at the particular nozzle-inlet condition (P_1 and T_1). When the critical-pressure relation (equation (3)) is substituted in equations (9) and (12) and similar terms are grouped, the critical-flow condition is

$$V_{i,2}'=\sqrt{2gJc_pT_1\frac{\gamma-1}{\gamma+1}} \tag{14}$$

and

$$W_i'=A_2V_{i,2}'\frac{P_1}{RT_1}\left(\frac{2}{\gamma+1}\right)^{\frac{1}{\gamma-1}} \tag{15}$$

A simplification of the thrust calculation for supercritical pressure ratios (equation (13)) can be obtained if the calculated pressure term is dropped and the thrust calculation is based on an effective jet velocity V_e:

$$F_j=\frac{W_m}{g}V_{e,2}$$
$$=C_d\frac{W_i'}{g}C_{v,e}V_{i,2} \tag{16}$$

The theoretical velocity is based on the assumption of complete isentropic expansion to atmospheric pressure even though the pressure ratio across the nozzle may exceed the critical pressure ratio. The theoretical velocity may be calculated from equation (9) with $p_2=p_0$. The effective velocity coefficient $C_{v,e}$ from equation (16) is

$$C_{v,e}=\frac{V_e}{V_i} \tag{17}$$

Values of both C_v and $C_{v,e}$ are presented. For convenience, C_v will be designated the velocity coefficient and $C_{v,e}$ the effective velocity coefficient. Below the critical pressure ratio, p_2 is equal to p_0, which makes the two velocity coefficients equal from the equality of equations (13) and (16).

The Reynolds numbers were calculated using the nozzle-outlet diameter in the following equation:

$$Re=\frac{\rho_2 V_2 D_2}{\mu_2} \tag{18}$$

The Mach numbers were calculated for two values of γ by

$$M=\sqrt{\frac{2}{\gamma-1}\left[\left(\frac{P_1}{p_0}\right)^{\frac{\gamma-1}{\gamma}}-1\right]} \tag{19}$$

APPARATUS AND PROCEDURE

The apparatus used is diagrammatically shown in figure 1. The air flow, supplied to the apparatus at approximately

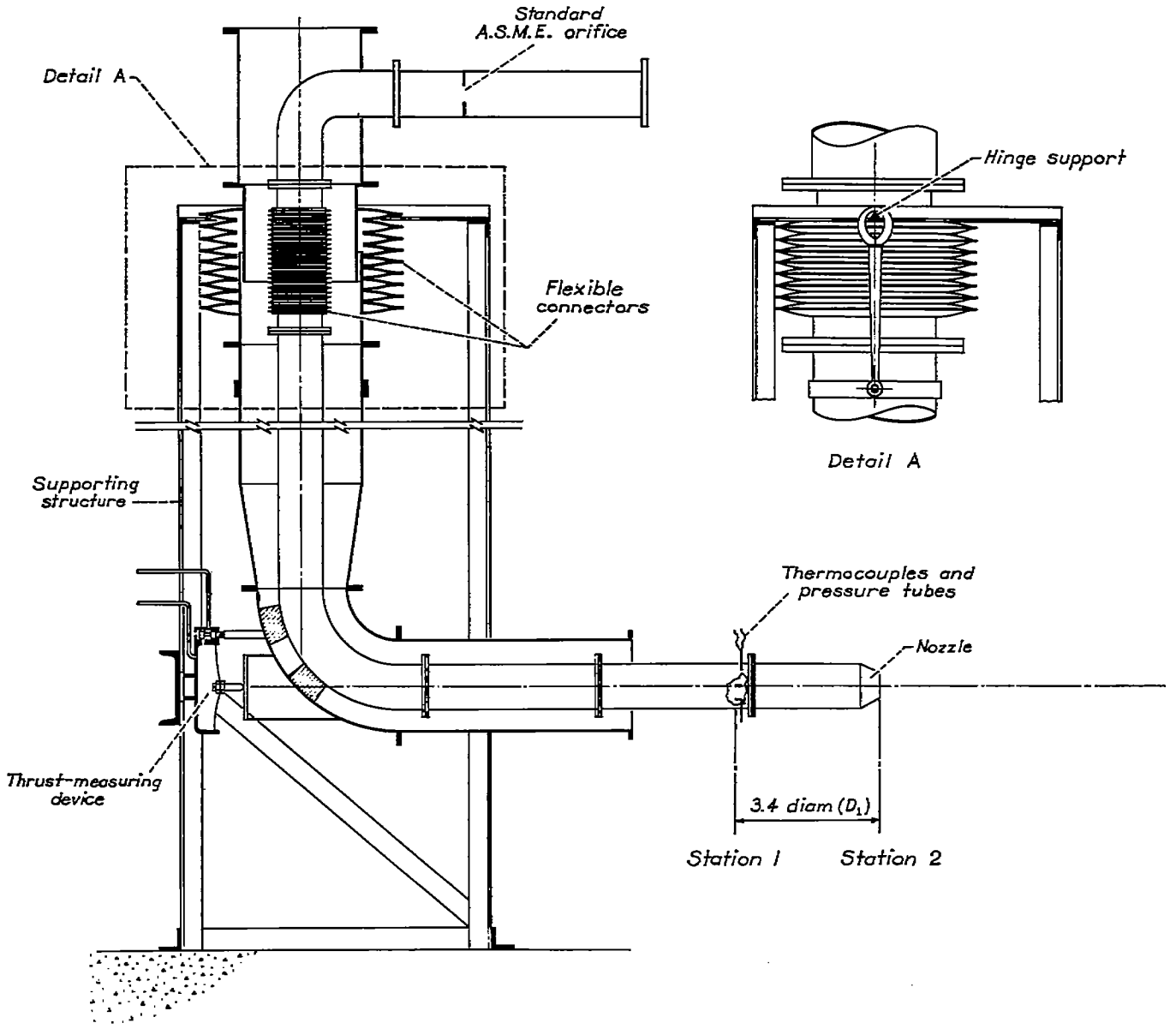

FIGURE 1.—Diagrammatic sketch of apparatus

80° F, was determined by use of a standard A.S.M.E. orifice (reference 1). The apparatus was attached to the air-supply system through flexible metal bellows to allow the apparatus to swing freely from a hinged joint, so that thrust could be directly measured; a balanced-pressure diaphragm-type thrust indicator was used.

The nozzle-inlet instrumentation (station 1) consisted of two unshielded iron-constantan thermocouples, two total-pressure tubes, and two static-pressure tubes. The minimum distance between the nozzle outlet and the inlet instrumentation was greatest for the 5° nozzle, with a diameter ratio of 0.50. The distance required in this installation, 3.4 inlet diameters, was used for all installations. The instrumentation was placed at a distance from the wall of 20 percent of the radius. This distance was determined by investigation with rake surveys at station 1 in order to obtain true average readings. By using these readings, air flow that agreed within 1 percent of the orifice-measured air flow was computed.

All nozzles were of welded 16-gage sheet steel with an inlet diameter of 5 inches. Nozzles deviated somewhat from design dimensions in some cases as can be seen in table I, which gives the nozzle configurations and measurements. Because of the deviations in dimensions, the data were cross-plotted to obtain data corresponding to the same angles for each of the diameter ratios investigated.

All nozzles were investigated by varying only the nozzle-inlet total pressure, which could be measured directly within ±0.05 inch of mercury.

The indicated temperature T_i measured at station 1 was corrected to total temperature. The nozzle-inlet indicated temperature is a measure of the static temperature plus a portion of the stagnation-temperature rise; the general equation is

$$T_i = t + \beta\left(\frac{V^2}{2gJc_p}\right) \tag{20}$$

From calibration tests of thermocouples of the type used, the impact-recovery factor β was found to equal 0.80. With the value of β known, the nozzle-inlet total temperature T_1 can be calculated from indicated temperatures by the general equation

$$T = \frac{T_i}{1+(1-\beta)\left[\left(\frac{p}{P}\right)^{\frac{\gamma-1}{\gamma}}-1\right]} \tag{21}$$

Inasmuch as the temperature of the working fluid was nearly the same as that of the surroundings, the radiation and conduction losses from the thermocouples were considered negligible.

RESULTS AND DISCUSSION

FLOW SIMILARITY

In order that the data obtained on the 5-inch nozzles can be directly applied to full-scale jet-engine nozzle design and performance, flow similarity must be established between the model and full-scale nozzles. The predominant factors for flow similarity are geometric similarity, Reynolds number, and Mach number. The geometric similarity is satisfied by selection of the proper model nozzle for comparison.

The range and the comparison of Reynolds number is shown in figure 2. The range of Reynolds numbers for the model

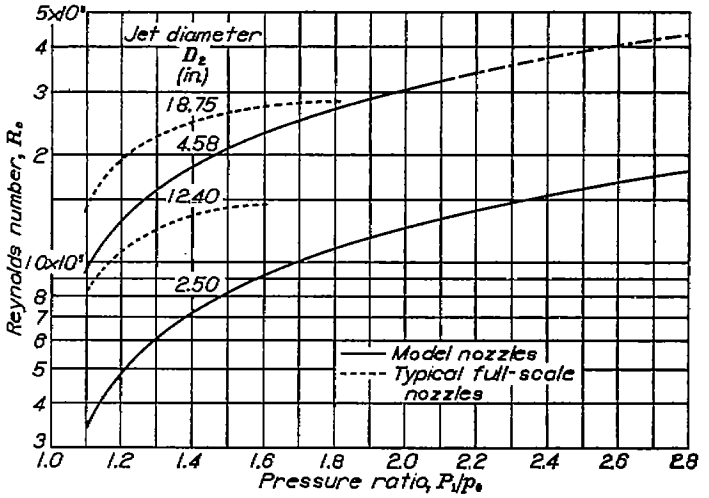

FIGURE 2.—Range and comparison of Reynolds number for model and full-scale nozzles over range of pressure ratios.

nozzles is approximately between 3×10^5 and 4×10^6. The range of Reynolds numbers for typical full-scale jet-engine nozzles is between 8×10^5 and 3×10^6. The effects of Reynolds numbers were not investigated. Inasmuch as the range of Reynolds numbers of the model and typical full-scale nozzles is of approximately the same order of magnitude, the difference in Reynolds number is considered negligible in the application of the model data to full-scale-nozzle design and performance.

The comparison of Mach number for two values of ratio of specific heats γ plotted against pressure ratio is shown in figure 3. The value of γ for the model nozzles is approxi-

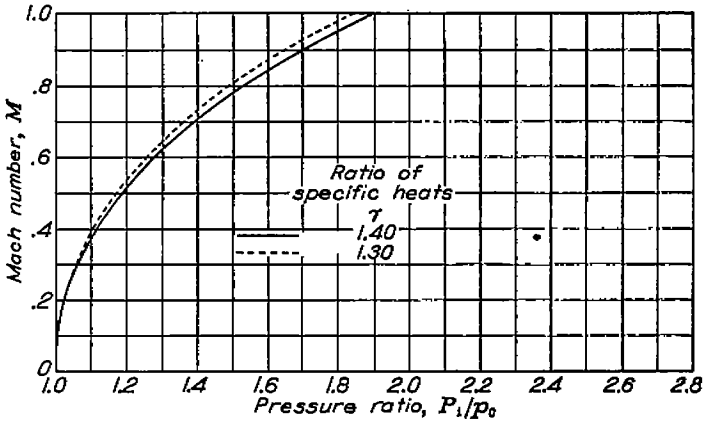

FIGURE 3.—Comparison of Mach number for two values of ratio of specific heats over range of pressure ratios. (γ for model nozzles, approximately 1.40; γ for full-scale nozzles, 1.30 to 1.40.)

mately 1.40 and the value of γ for typical full-scale jet-engine nozzles is between 1.30 and 1.40. For test conditions of equal Mach number, the difference in pressure ratio is small. This small difference in pressure ratios will be shown in the following section to have very little effect on the nozzle coefficients. From the foregoing analysis, flow similarity between the model and full-scale nozzles appears to have been satisfied

with reasonable accuracy and the results of the model tests are considered directly applicable to full-scale-nozzle design and performance.

FLOW COEFFICIENT

The effects on nozzle performance of changes in diameter ratio, cone angle, and pressure ratio are presented. Figure 4 shows the measured effects of change in pressure ratio on the performance of all nozzles investigated. For all nozzles, the flow coefficient increased with an increase in pressure ratio. Also a rapid decrease in flow coefficient with increasing nozzle cone angle can be seen.

Values of flow coefficient for nozzles with cone angles of 5°, 15°, 30°, 45°, and 90° were obtained from cross-plotting values of flow coefficient obtained from figure 4 against the nozzle cone angle for each diameter ratio. These data were

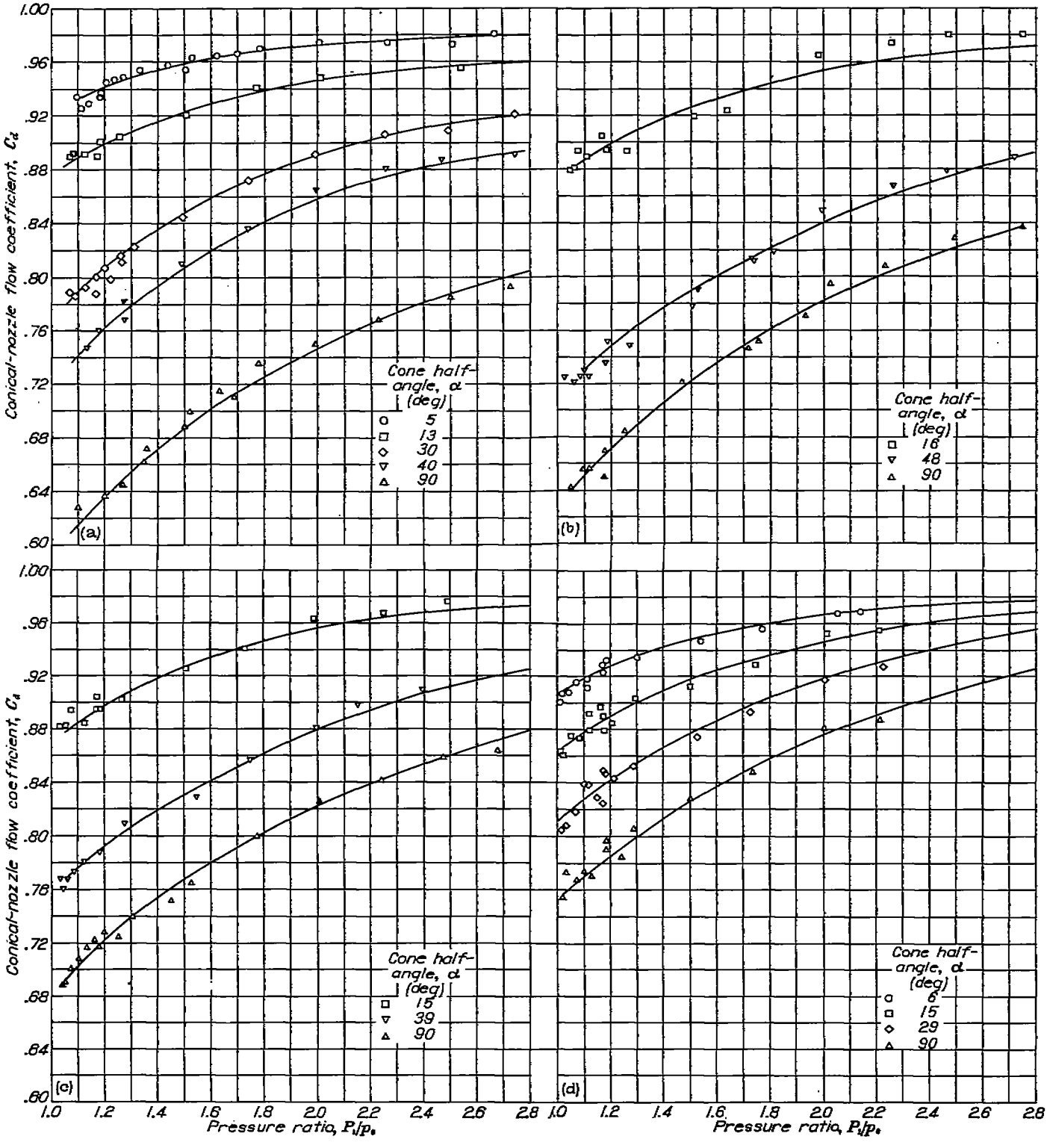

(a) Outlet-inlet diameter ratio, 0.50.
(b) Outlet-inlet diameter ratio, 0.67.
(c) Outlet-inlet diameter ratio, 0.80.
(d) Outlet-inlet diameter ratio, 0.91.

FIGURE 4.—Variation of conical-nozzle flow coefficient with pressure ratio across nozzle for various cone half-angles.

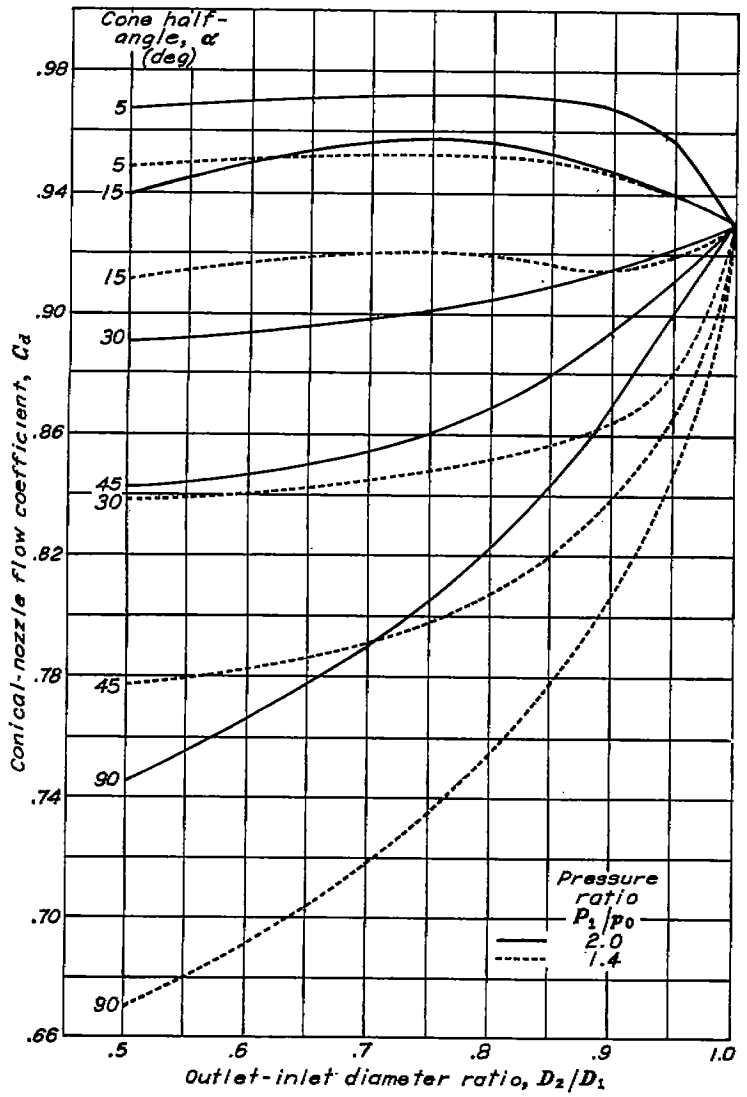

FIGURE 5.—Variation of conical-nozzle flow coefficient with outlet-inlet diameter ratio for nozzles with various cone half-angles at two pressure ratios.

again cross-plotted (fig. 5) to show variations in flow coefficient with changes in diameter ratio for pressure ratios of 2.0 and 1.4. The nozzles with small cone angles reach an optimum diameter ratio of about 0.75. At a pressure ratio of 2.0, a maximum flow coefficient of 0.972 is indicated for the 5° nozzle. In general, the flow coefficient for nozzles with large cone half-angles increases with increasing diameter ratio. The curves for all nozzles approach a particular value of flow coefficient at a diameter ratio of 1.0 because this value represents a straight length of pipe. The flow coefficient for a straight length of pipe is shown in figure 6.

The variations in flow coefficients for nozzles of various cone angles with changes in area ratio A_2/A_1 over a range of

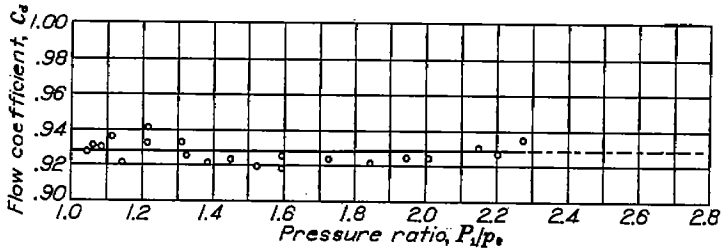

FIGURE 6.—Variation in flow coefficient with pressure ratio for discharge from straight pipes.

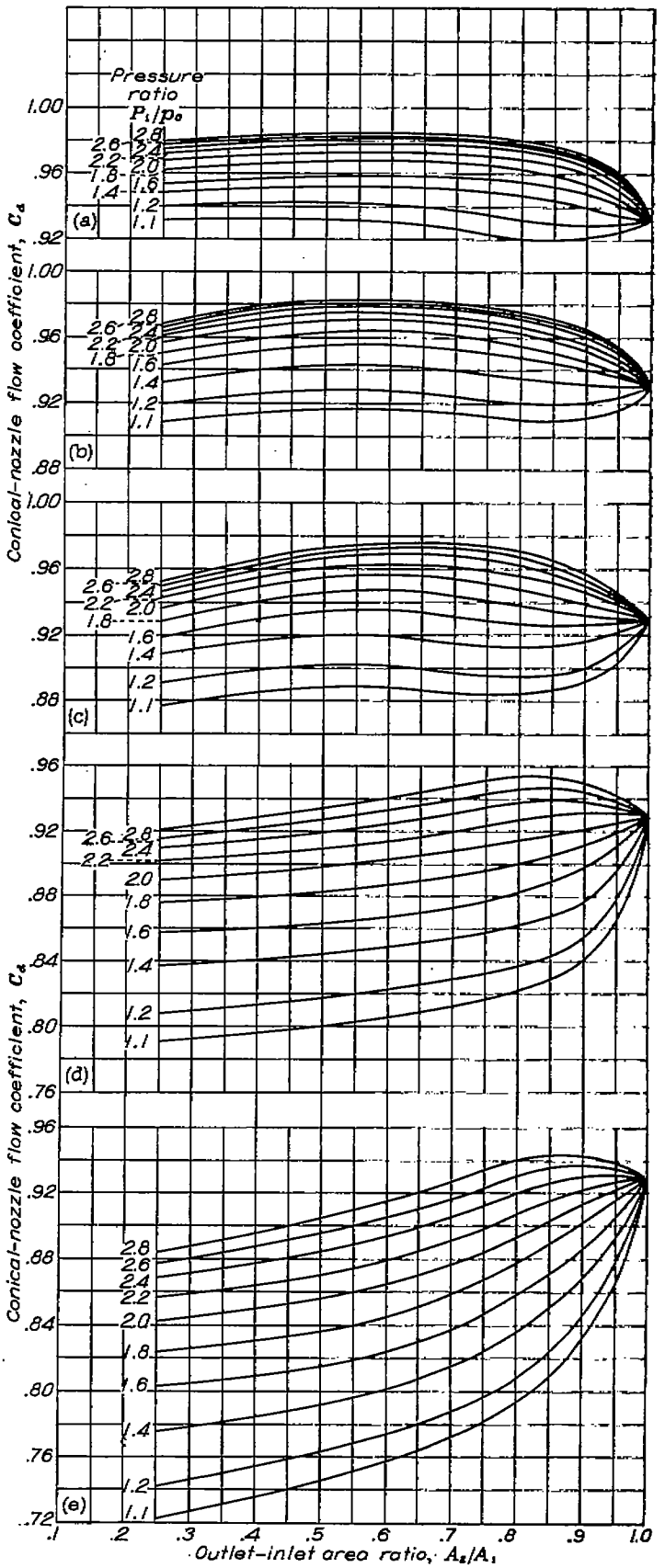

(a) Cone half-angle, 5°.
(b) Cone half-angle, 10°.
(c) Cone half-angle, 15°.
(d) Cone half-angle, 30°.
(e) Cone half-angle, 45°.

FIGURE 7.—Variation of conical-nozzle flow coefficient with outlet-inlet area ratio for various pressure ratios.

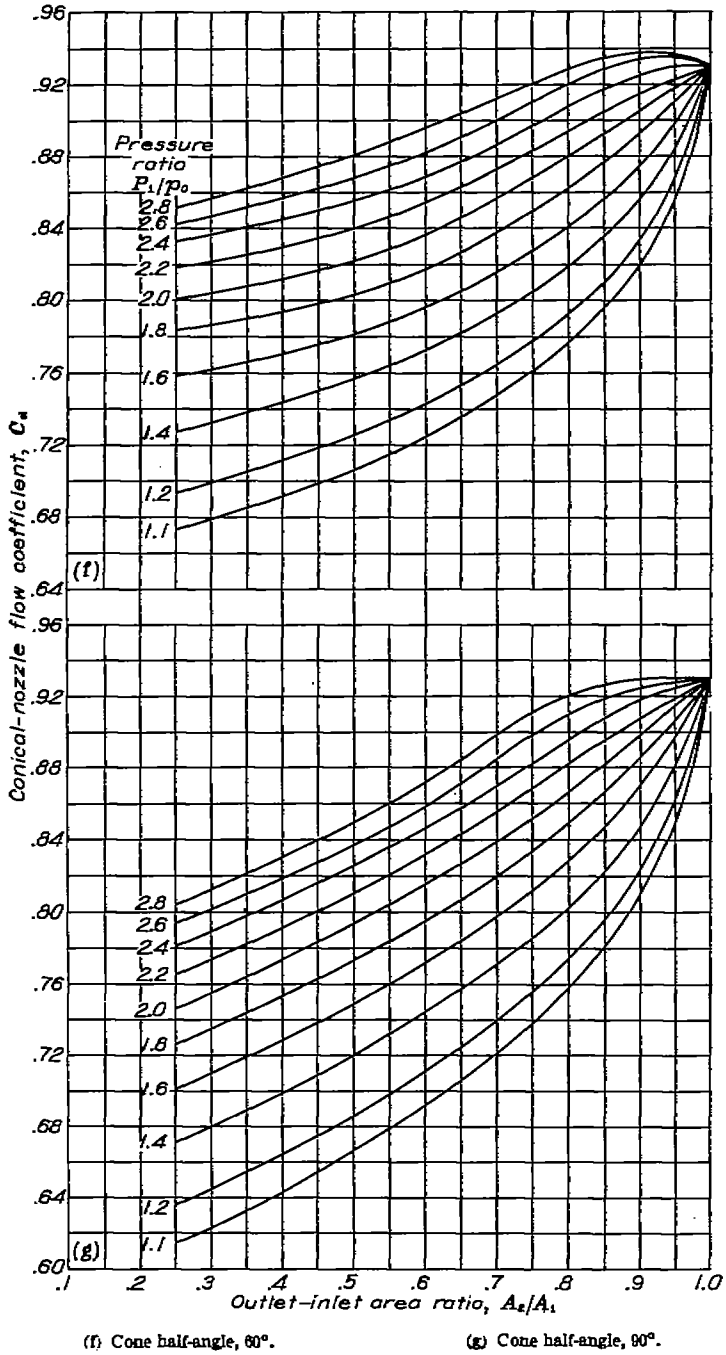

(f) Cone half-angle, 60°. (g) Cone half-angle, 90°.

FIGURE 7.—Concluded. Variation of conical-nozzle flow coefficient with outlet-inlet area ratio for various pressure ratios.

pressure ratios are presented in figure 7. The maximum values of the flow coefficients mentioned in the discussion of figure 5 are better seen in figures 7(a), 7(b), and 7(c) for cone half-angles of 5°, 10°, and 15°, respectively. Figure 7 presents the data in the most convenient form for use in design of conical nozzles. The use of area ratio instead of diameter ratio for these charts simplifies the selection of a nozzle to give a desired flow rate.

VELOCITY COEFFICIENT

The velocity coefficients C_v are given for all nozzles in figure 8. One value of velocity coefficient, 0.945, represents the data obtained with all nozzles within ±0.03, between pressure ratios of 1.3 and the critical value (approximately 1.9). The scatter of the data due to inaccuracies in the measurements of flow and thrust at pressure ratios below 1.3 was great enough to obscure any trend of the nozzle performance at the very low pressure ratios. At supercritical pressure ratios, the velocity coefficient decreased to a value of 0.893 at a pressure ratio of approximately 2.8. The mean curve represents the supercritical data within ±0.03. The velocity coefficient was essentially independent of cone angle and diameter ratio and dependent only on pressure ratio.

The effective velocity coefficients $C_{v,e}$ (fig. 9) are used only for the simplified thrust calculations for all the nozzles investigated. One value of effective velocity coefficient, 0.945, represents the data obtained with all nozzles within ±0.03 between pressure ratios of 1.3 and the critical value. This value is the same as that obtained for the velocity coefficient of figure 8, because the velocity coefficient and the effective velocity coefficient are identical in the subcritical-pressure-ratio operating range. At supercritical pressure ratios, the average value of effective velocity coefficient decreases slightly to 0.934 at a pressure ratio of approximately 2.8.

COMPARISON OF THRUST PERFORMANCE

The variation in thrust with change in pressure ratio is a function of only the flow coefficients and exit areas, as can be demonstrated:

From equation (16)

$$\frac{F_{j,x}}{F_{j,y}}=\frac{C_{d,x}W_{i,x}C_{v,e,x}V_{i,x}}{C_{d,y}W_{i,y}C_{v,e,y}V_{i,y}} \tag{22}$$

The velocities are functions of only pressure ratio and initial temperature (equation (9)) and at any particular operating condition are therefore equal. The velocity co-

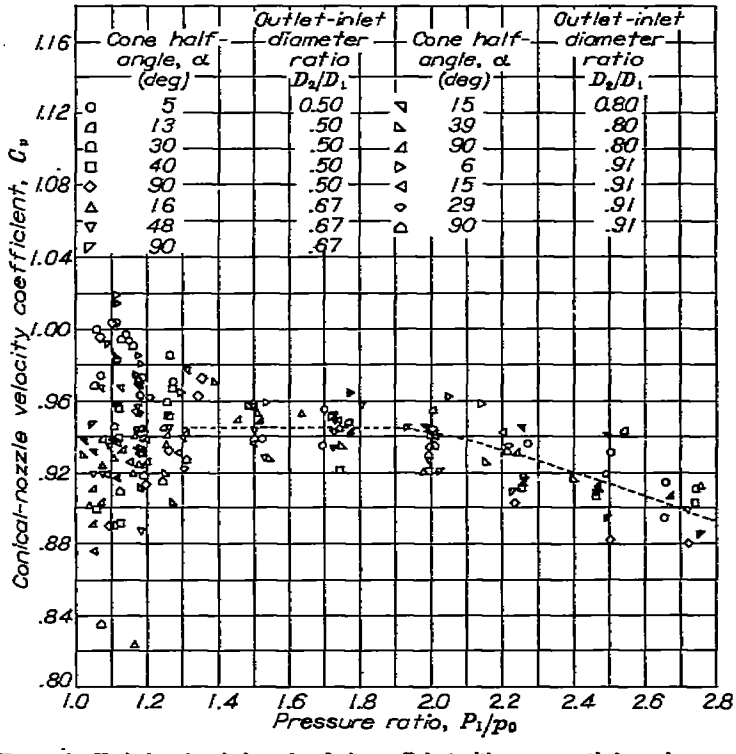

FIGURE 8.—Variation of conical-nozzle velocity coefficient with pressure ratio for various cone half-angles and outlet-inlet diameter ratios.

efficients are also equal because they are a function of only pressure ratio (fig. 9). The air-flow ratio $W_{t,x}/W_{t,y}$ is equal to the ratio of outlet areas for any particular operating condition. (See equation (12).) The thrust ratio may be written as

$$\frac{F_{t,x}}{F_{t,y}}=\frac{C_{d,x}A_{2,x}}{C_{d,y}A_{2,y}} \tag{23}$$

Inasmuch as the exit areas are fixed, the ratio of performance (air flow and thrust) of nozzles of different design selected for the same thrust at a particular condition is proportional to the ratio of flow coefficients.

Thrust with the 90° and 5° nozzles is compared in figure 10 over a range of pressure ratios between approximately 1.0 and 2.8. These two nozzles were designed to give the same thrust (effective flow area and air flow) at a pressure ratio of 2.0 and were chosen to show the maximum variation in thrust. The variation in thrust between the two nozzles with increasing pressure ratio results from the larger outlet area of the 90° nozzle and a more rapid increase in flow coefficient than for the 5° nozzle. The thrust ratio increases for the 90° nozzle with an increase in pressure ratio above the design pressure ratio because of the greater effective flow area, and decreases with a decrease in pressure ratio because of the smaller effective flow area.

SUMMARY OF RESULTS

From an investigation of conical jet nozzles with inlet diameters of 5 inches, outlet-inlet diameter ratios from 0.50 to 0.91, and cone half-angles from 5° to 90° at pressure ratios from 1.0 to 2.8, the following performance characteristics were determined:

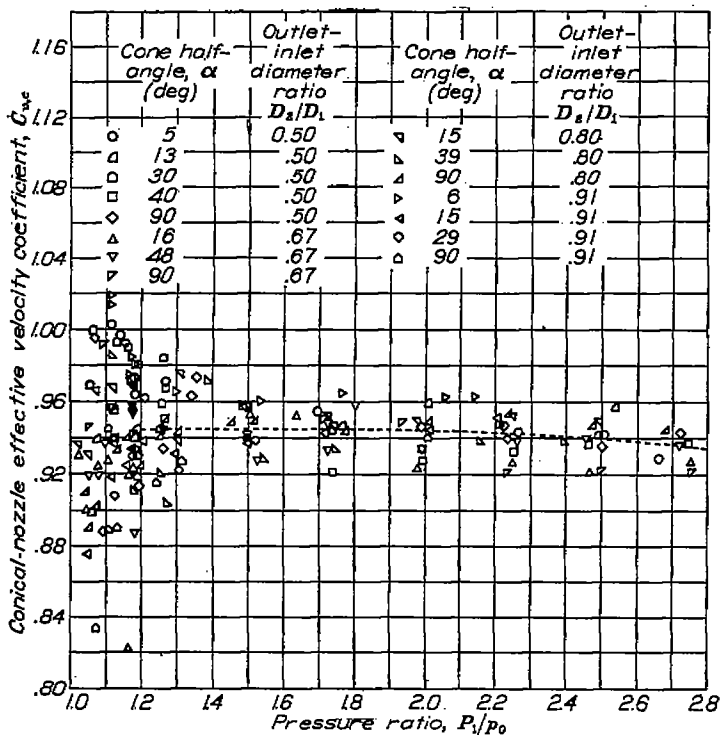

FIGURE 9.—Variation of conical-nozzle effective velocity coefficient with pressure ratio for various cone half-angles and outlet-inlet diameter ratios (used only for simplification of thrust calculations).

1. The flow coefficient for all nozzles increased with increasing pressure ratio.

2. The flow coefficient for all nozzles increased with decreasing cone half-angle.

3. The flow coefficient of nozzles with small cone half-angles reached an optimum at a diameter ratio of about 0.75. The flow coefficient of nozzles with large cone half-angles in general increased with increasing diameter ratio.

4. The velocity coefficient could be reasonably well represented by a value of 0.945 in the range of pressure ratios from 1.3 to the critical pressure ratio. At pressure ratios above the critical value, the velocity coefficient decreased to a value of 0.893 at a pressure ratio of 2.8.

5. The velocity coefficient was essentially independent of cone half-angle and of outlet-inlet diameter ratio.

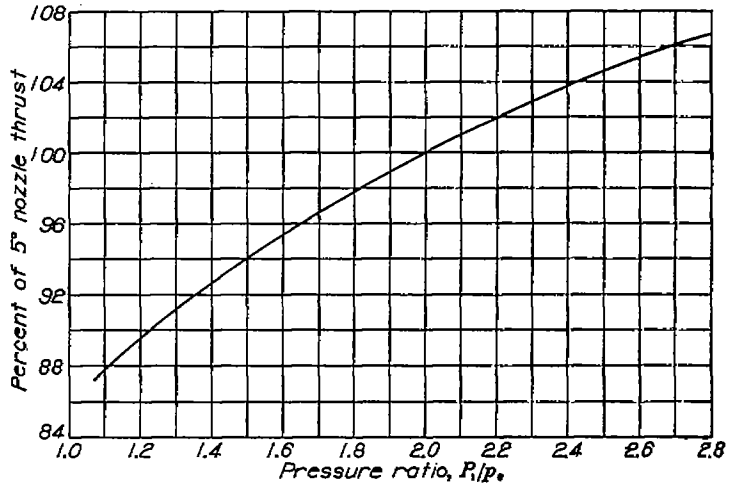

FIGURE 10.—Comparison of thrust of 90° nozzle with that of 5° nozzle at various pressure ratios. (Design points, P_1/p_0, 2.0; A_2/A_1 of 90° nozzle, 0.596; A_2/A_1 of 5° nozzle, 0.490.)

6. The effective velocity coefficient was based on the assumption of complete isentropic expansion to ambient pressure when the nozzle is operated above the critical pressure ratio, and was identical with the velocity coefficient below the critical pressure ratio. Above the critical pressure ratio, the effective velocity coefficient decreased from 0.945 to 0.934 at a pressure ratio of 2.8.

7. The comparative performances (thrust and air flow) of nozzles selected for the same performance at a particular design condition were proportional to the ratio of their flow coefficients because the velocity coefficient is essentially independent of nozzle design.

LEWIS FLIGHT PROPULSION LABORATORY,
NATIONAL ADVISORY COMMITTEE FOR AERONAUTICS,
CLEVELAND, OHIO, *September 7, 1948.*

REFERENCE

1. Anon.: Flow Measurement 1940. A.S.M.E. Power Test Codes (Instruments and Apparatus Sec.), pub. by Am. Soc. Mech. Eng. (New York), 1940.

TABLE I—NOZZLE CONFIGURATIONS AND MEASUREMENTS

[Cone half-angle α measured at 90° intervals around periphery; outlet diameter D_2 measured at 60° intervals around periphery; inlet diameter D_1 of all nozzles, 5 in.]

Configuration	Measurement	Cone half-angle α, (deg)	Outlet diameter D_2, (in.)	Diameter ratio D_2/D_1
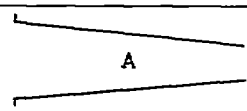 A	1	5.8	2.515	0.5030
	2	4.0	2.528	.5056
	3	5.5	2.494	.4988
	4	4.5	-----	------
	Av	5.0	2.512	.5024
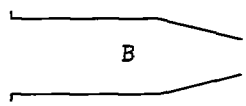 B	1	14.0	2.495	0.4990
	2	14.5	2.524	.5048
	3	13.0	2.490	.4980
	4	12.0	-----	------
	Av	13.4	2.503	.5006
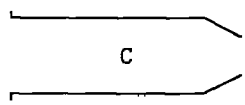 C	1	31.0	2.504	0.5008
	2	29.0	2.500	.5000
	3	30.8	2.501	.5002
	4	29.0	-----	------
	Av	30.0	2.502	.5004
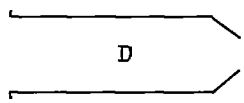 D	1	39.5	2.499	0.4998
	2	40.5	2.513	.5026
	3	39.0	2.493	.4986
	4	40.8	-----	------
	Av	40.0	2.502	.5004
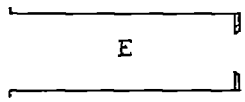 E	1	90.0	2.500	0.5000
	2	90.0	2.500	.5000
	3	90.0	2.500	.5000
	4	90.0	-----	------
	Av	90.0	2.500	.5000
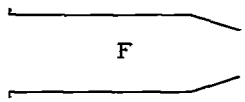 F	1	15.5	3.312	0.6624
	2	16.5	3.318	.6636
	3	16.3	3.378	.6756
	4	15.0	-----	------
	Av	15.8	3.336	.6672
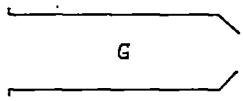 G	1	47.7	3.367	0.6734
	2	48.7	3.351	.6702
	3	47.9	3.337	.6674
	4	47.9	-----	------
	Av	48.0	3.352	.6704
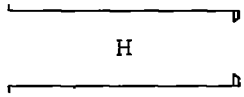 H	1	90.0	3.333	0.667
	2	90.0	3.333	.667
	3	90.0	3.333	.667
	4	90.0	-----	------
	Av	90.0	3.333	.667
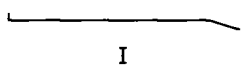 I	1	14.2	3.995	0.7990
	2	15.2	4.014	.8028
	3	14.8	3.985	.7970
	4	15.8	-----	------
	Av	15.0	3.998	.7996
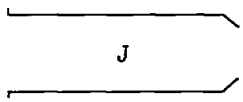 J	1	38.5	3.990	0.7980
	2	38.5	3.985	.7970
	3	39.5	3.998	.7992
	4	39.0	-----	------
	Av	38.9	3.990	.7980
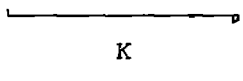 K	1	90.0	4.000	0.8000
	2	90.0	4.000	.8000
	3	90.0	4.000	.8000
	4	90.0	-----	------
	Av	90.0	4.000	.8000
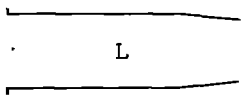 L	1	6.0	4.570	0.9140
	2	6.0	4.552	.9104
	3	5.3	4.580	.9160
	4	6.2	-----	------
	Av	5.9	4.567	.9134
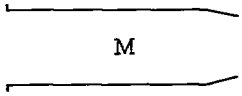 M	1	14.8	4.528	0.9056
	2	15.0	4.496	.8992
	3	14.8	4.519	.9038
	4	15.0	-----	------
	Av	14.9	4.514	.9028
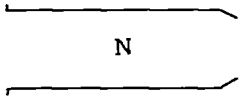 N	1	29.5	4.531	0.9062
	2	29.0	4.538	.9076
	3	29.5	4.550	.9100
	4	28.5	-----	------
	Av	29.1	4.540	.9080
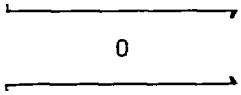 O	1	90.0	4.545	0.9090
	2	90.0	4.545	.9090
	3	90.0	4.545	.9090
	4	90.0	-----	------
	Av	90.0	4.545	.9090